JACC: CARDIOVASCULAR INTERVENTIONS
VOL. 5, NO. 4, 2012

ISSN 1936-8798/$36.00
PUBLISHED BY ELSEVIER INC.
DOI: 10.1016/j.jcin.2011.12.015

Differences in Neointimal Thickness Between the Adluminal and the Abluminal Sides of Malapposed and Side-Branch Struts in a Polylactide Bioresorbable Scaffold

Evidence In Vivo About the Abluminal Healing Process

Juan Luis Gutiérrez-Chico, MD, PHD,* Frank Gijsen, MSC, PHD,†
Evelyn Regar, MD, PHD,* Jolanda Wentzel, MSC, PHD,† Bernard de Bruyne, MD, PHD,‡
Leif Thuesen, MD,§ John Ormiston, MD,‖ Dougal R. McClean, MD,¶
Stephan Windecker, MD,# Bernard Chevalier, MD,** Dariusz Dudek, MD, PHD,††
Robert Whitbourn, MD,‡‡ Salvatore Brugaletta, MD,* Yoshinobu Onuma, MD,*
Patrick W. Serruys, MD, PHD*

Rotterdam, the Netherlands; Aalst, Belgium; Aarhus, Denmark; Grafton-Auckland and Christchurch, New Zealand; Bern, Switzerland; Massy, France; Krakow, Poland; and Melbourne, Australia

Objectives The goal of this study was to describe the neointimal healing on the abluminal side (ABL) of malapposed (ISA) struts and nonapposed side-branch (NASB) struts in terms of coverage by optical coherence tomography (OCT) and in comparison with the adluminal side (ADL).

Background The neointimal healing on the ABL of ISA and NASB struts has never to our knowledge been explored in vivo and could be involved in the correction of acute malapposition. The bioresorbable vascular scaffold (BVS) is made of a translucent polymer that enables imaging of the ABL with OCT.

Methods Patients enrolled in the ABSORB B (ABSORB Clinical Investigation Cohort B) study were treated with implantation of a BVS and imaged with OCT at 6 months. Thickness of coverage on the ADL and ABL of ISA and NASB struts was measured by OCT.

Results Twenty-eight patients were analyzed; 114 (2.4%) struts were malapposed or at side branches. In 76 ISA struts (89.4%) and 29 NASB struts (100%), the thickness of ABL coverage was >30 μm. Coverage was thicker on the ABL than on the ADL side (101 vs. 71 μm; 95% confidence interval [CI] of the difference: 20 to 40 μm). In 70 struts (60.7%, 95% CI: 50.6% to 70.0%), the neointimal coverage was thicker on the ABL, versus only 20 struts (18.5%, 95% CI: 11.6% to 28.1%) with thicker neointimal coverage on the ADL side (odds ratio: 3.35, 95% CI: 2.22 to 5.07).

Conclusions Most of the malapposed and side-branch struts are covered on the ABL side 6 months after BVS implantation, with thicker neointimal coverage than on the ADL side. The physiological correction of acute malapposition involves neointimal growth from the strut to the vessel wall or bidirectional. (ABSORB Clinical Investigation, Cohort B [ABSORB B]; NCT00856856) (J Am Coll Cardiol Intv 2012;5:428–35) © 2012 by the American College of Cardiology Foundation

From the *Interventional Cardiology Department, Erasmus Medical Centre, Thoraxcentre, Rotterdam, the Netherlands; †Biomedical Engineering Department, Erasmus Medical Centre, Thoraxcentre, Rotterdam, the Netherlands; ‡Interventional Cardiology Department, Onze Lieve Vrouw Ziekenhuis, Aalst, Belgium; §Interventional Cardiology Department, Skejby

The neointimal healing process after stenting has been extensively studied in the bare-metal stent (BMS) era, to understand the mechanisms of restenosis. Experimental studies have described proliferation of endothelial and smooth muscle cells after endothelial denudation (1–4), starting from the noninjured segments, until the endothelial continuity is restored (5–9). At this point, the confluence of endothelial cells inhibits their own proliferation and stimulates the secretion of heparin-sulfates, inhibiting in turn the proliferation of smooth muscle cells (10). According to this confluent model, in case of detachment of struts from the vessel wall, the endothelial cells can spread on the surface of the stent until the contact with other endothelial cells stops the process, thus resulting in conformal coverage of the whole detached mesh. As an additional mechanism, circulating endothelial progenitor cells enhance re-endothelialization (11,12).

The interest to study the neointimal healing has grown exponentially in the drug-eluting stent (DES) era. Pathology studies described the association between delayed neointimal healing and very late stent thrombosis in DES (13–16). As a consequence, imaging techniques such as angioscopy (17–19) or optical coherence tomography (OCT) (20–24) have tried to estimate the degree of neointimal coverage in clinical series, exploring its value as a potential surrogate for thrombotic events. However, our knowledge about the healing process is limited to the adluminal (ADL) side of the struts. Pathology studies have paid little attention to the abluminal (ABL) side of malapposed or side-branch struts, probably due to the scarce information available about these specific categories and to methodological challenges for an accurate assessment. The ABL side has remained inaccessible in vivo also for angioscopy and OCT. OCT has become an experimental tool for the assessment of coverage due to a 10-fold higher axial resolution (14 μm) than intravascular ultrasound (IVUS), but the intense optical backscattering at the surface of metallic struts casts a dorsal shadow that prevents ABL visualization. The healing process on the ABL side might play a relevant role in the spontaneous resolution of acute incomplete stent apposition (ISA), as described in recent sequential OCT studies (24–26). Conversely to DES, the bioresorbable vascular scaffold (BVS) is made of a translucent polymer, resulting in significant backscattering of the optical radiation only at the strut boundaries and no dorsal shadowing, thus enabling for the first time quantification of the neointimal thickness on the ABL side of those struts detached from the vessel wall. In this study, we compare the neointimal thickness on the ABL versus ADL sides of ISA and nonapposed side-branch (NASB) struts in the BVS.

Methods

BVS technical specifications. BVS (Abbott Vascular) is a fully bioresorbable scaffold, consisting of a semicrystalline poly-L-lactide (PLLA) backbone, coated by a thin amorphous layer of poly-D,L-lactide (PDLLA) containing the antiproliferative agent everolimus. BVS struts have a total thickness of 150 μm and are fully resorbed 2 years after implantation (27), following a process in which the long chains of PLLA and PDLLA are progressively cleaved as ester bonds between lactide repeating units are hydrolyzed. Eventually, small particles <2 μm in diameter are phagocytosed by macrophages. Ultimately, PLLA and PDLLA degrade to lactate, which is metabolized via the Krebs cycle. The whole scaffold is translucent to optical radiation, with the exception of 2 radio-opaque platinum markers embedded into the proximal and distal edges, to ease fluoroscopic visualization. BVS has proved excellent clinical and angiographic results up to 2-years follow-up, at which time the scaffold is resorbed (27,28).

Abbreviations and Acronyms

ABL = abluminal
ADL = adluminal
BMS = bare-metal stent(s)
BVS = bioresorbable vascular scaffold
CI = confidence interval
DES = drug-eluting stent(s)
ISA = incomplete stent apposition
IVUS = intravascular ultrasound
NASB = nonapposed side branch
OCT = optical coherence tomography
PDLLA = poly-D,L-lactide
PLLA = poly-L-lactide
SS = sheer stress

Study sample. The ABSORB Cohort B registry (ABSORB Clinical Investigation Cohort B, NCT00856856) enrolled

Sygehus, Aarhus, Denmark; ‖Interventional Cardiology Department, Auckland City Hospital, Grafton-Auckland, New Zealand; ¶Interventional Cardiology Department, Christchurch Hospital, Christchurch, New Zealand; #Department of Cardiology, Swiss Heart Centre, Inselspital, Bern, Switzerland; **Interventional Cardiology Department, Institute Hospitalier Jacques Cartier, Massy, France; ††Interventional Cardiology Department, University Hospital Krakow, Krakow, Poland; and the ‡‡Interventional Cardiology Department, Saint Vincent's Hospital, Melbourne, Australia. This study has been sponsored by Abbott Vascular, Santa Clara, California. The core laboratory and contract research organization responsible for the analysis (Cardialysis BV, Rotterdam) and the participating centers (except the Biomedical Engineering Department, Erasmus Medical Centre, Thoraxcentre, Rotterdam, the Netherlands) have received grants from the sponsor to run the trial. Drs. de Bruyne, Thuesen, Ormiston, McClean, Windecker, Chevalier, Dudek, Whitbourn, and Serruys have received speakers' fees from the sponsor. Dr. Ormiston is on the advisory board for and received minor honoraria from Boston Scientific and Abbott Vascular. Dr. Windecker received research grants from Abbott, Boston Scientific, Biotronik, Biosensors, Cordis, and Medtronic. Dr. Chevalier is a consultant for Abbott Vascular. Dr. Dudek also has received research grants or served as consultant/advisory board member for Abbott, Adamed, AstraZeneca, Biotronik, Balton, Bayer, BBraun, BioMatrix, Boston Scientific, Boehringer Ingelheim, Bristol-Myers Squibb, Cordis, Cook, Eli Lilly, EuroCor, GlaxoSmithKline, Invatec, Medtronic, The Medicines Company, MSD, Nycomed, Orbus-Neich, Pfizer, Possis, Promed, Sanofi-Aventis, Siemens, Solvay, Terumo and Tyco. All other authors have reported that they have no relationships relevant to the contents of this paper to disclose. Patrick Whitlow, MD, served as Guest Editor for this paper.

Manuscript received August 23, 2011; revised manuscript received November 30, 2011, accepted December 1, 2011.

patients older than 18 years, with diagnosis of stable or unstable angina pectoris or silent ischemia, and de novo lesions in native coronary arteries amenable for percutaneous treatment with the BVS: % diameter stenosis ≥50% by visual estimation and reference vessel diameter of 2.5 to 3.5 mm. Major exclusion criteria were acute myocardial infarction, unstable arrhythmias, left ventricular ejection fraction ≤30%, restenotic lesions, lesions located in the left main coronary artery or in bifurcations involving a side branch >2 mm, a second clinically or hemodynamically significant lesion in the target vessel, documentation of intracoronary thrombus, or initial Thrombolysis In Myocardial Infarction flow grade 0. For invasive follow-up purposes, the cohort was subdivided into 2 groups: Cohort B1, undergoing multimodality invasive imaging (quantitative coronary angiography, IVUS, virtual histology, palpography, and OCT) at 6 and 24 months; and Cohort B2, with identical imaging follow-up protocol scheduled at 12 and 24 months. All the study lesions were treated with the BVS device revision 11 (3.0 × 18 mm). The registry was approved by the ethics committee at each participating institution, and each patient gave written informed consent before inclusion.

Table 1. Characteristics of the Different OCT Systems* in the Study, With the Corresponding Number of Patients Imaged by Each of Them

	M2	M3	C7
Technique	Occlusive	Nonocclusive	Nonocclusive
Domain	Time	Time	Fourier
Catheter*	ImageWire	ImageWire	Dragonfly
Rotation speed, frames/s	15.6	20	100
Pullback speed, mm/s	2	3	20
No. of patients	5	5	18

*All systems and catheters from LightLab Imaging, Westford, Massachusetts.
OCT = optical coherence tomography.

The present study analyzes the OCT images obtained 6 months after implantation from Cohort B1, when the structural integrity of the device is still preserved.

OCT study. OCT pullbacks were obtained with M2, M3, or C7 systems (LightLab Imaging, Westford, Massachusetts),

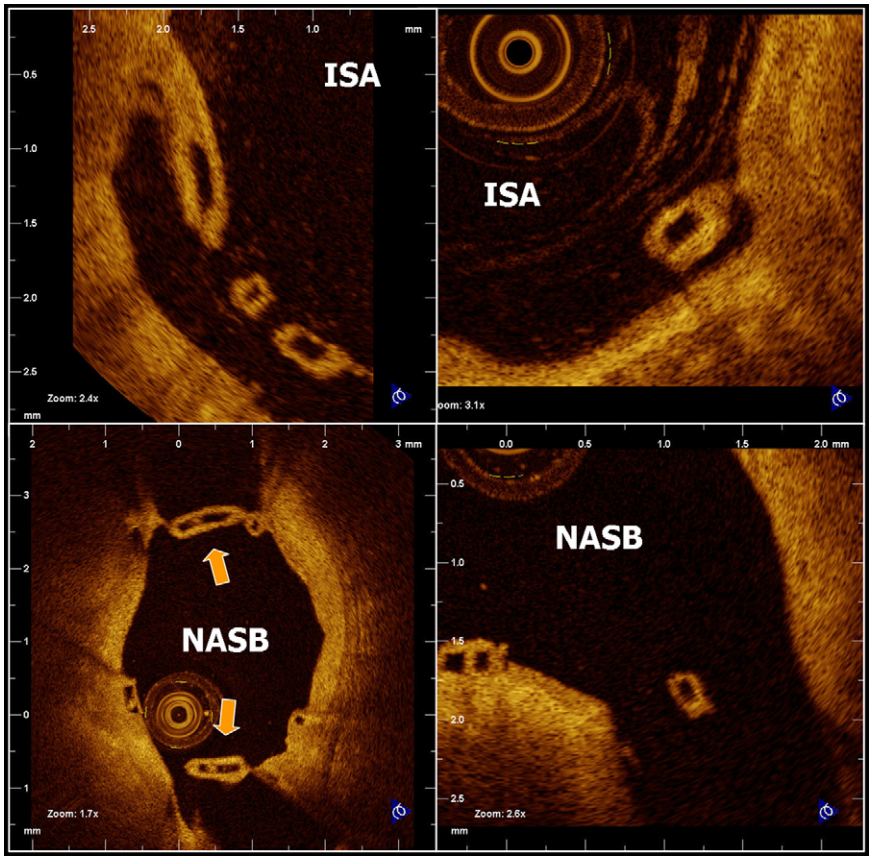

Figure 1. ISA and NASB Struts

Incomplete stent apposition (ISA) or malapposed struts are those separated from the vessel wall by a contrast-filled gap **(upper panels)**. The underlying vessel wall needs to be visible in the cross section to properly classify a strut as ISA. Nonapposed side-branch (NASB) struts are those located at the ostium of side branches, with no vessel wall behind **(lower panels, arrows)**. In NASB struts, apposition cannot be assessed by optical coherence tomography.

depending on the site, using an occlusive or nonocclusive technique, as appropriate (Table 1).

OCT images were analyzed offline in a core laboratory (Cardialysis BV, Rotterdam, the Netherlands) by independent investigators, using proprietary software (LightLab Imaging). Cross sections at 1-mm longitudinal intervals within the scaffolded segment and 5 mm proximal and distal to the scaffold edges were analyzed. Apposition was visually assessed strut by strut. Malapposition, also named incomplete stent apposition (ISA), was defined as a break in continuity between the backscattering frame of the translucent strut and the vessel wall, appearing as a contrast-filled gap between these 2 structures (Fig. 1). In the regions where ISA was found, cross sections at 0.2-mm longitudinal intervals were analyzed. Struts located at the ostium of side branches, with no vessel wall behind, were labeled as NASB struts and considered an independent category of apposition (Fig. 1).

Neointimal thickness was measured on both the ADL and ABL sides of each ISA or NASB strut as the distance from the black-box boundary to the neointima-lumen interface, following a straight line connecting the midpoint of the longitudinal axis of the strut with the center of gravity of the vessel (Fig. 2). Well-apposed struts were disregarded for this study. Previous analysis of 400 BVS struts immediately post-implantation reported an average thickness of 30.1 ± 5.7 μm for the ADL interface of the strut frame and 30.4 ± 5.7 μm for the ABL interface (the latter only accessible in 80 ISA or NASB struts) (29). On this basis, ABL neointimal thickness >30 μm or thicker than in the ADL side were both considered as highly suggestive of neointimal coverage.

Two independent analysts (J.L.G.C. and Y.O.) measured the thickness of coverage in the selected struts following the method described and blinded to one another's results, to assess interobserver reproducibility.

Statistical analysis. Coverage thickness on the ADL versus the ABL side of each strut was compared by multilevel linear regression with struts clustered at the patient level. The pooled percentages of struts with thicker ABL coverage and with

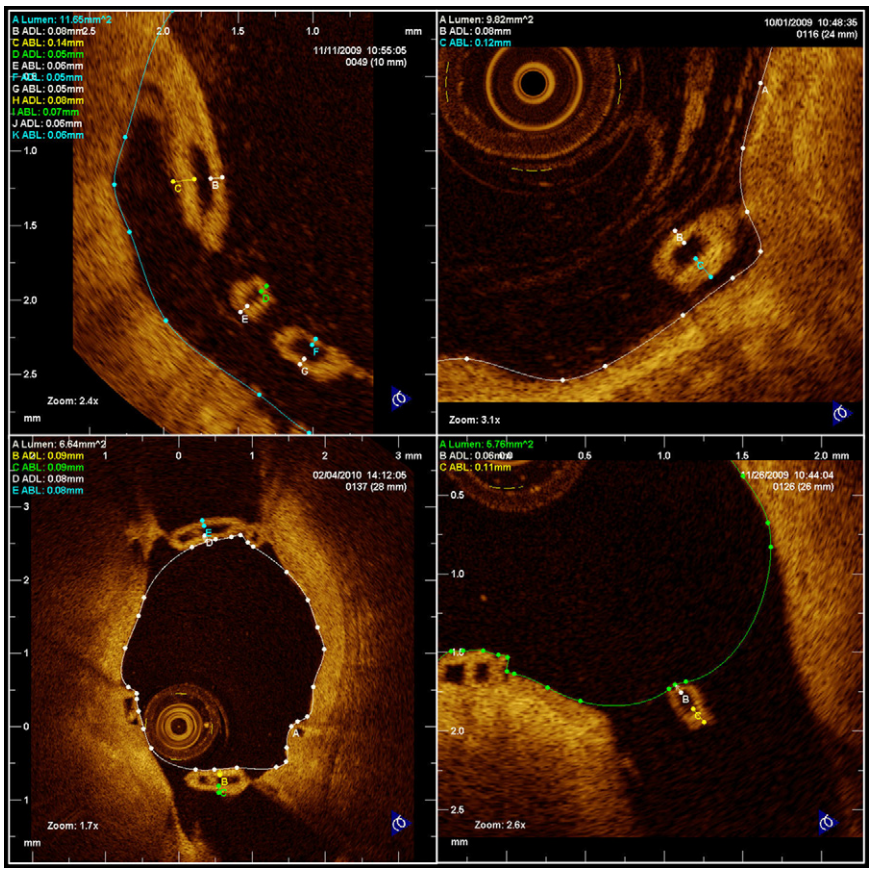

Figure 2. Measurement of Neointimal Thickness at the ADL and ABL Sides of ISA and NASB Struts

Measurement of neointimal thickness at the adluminal (ADL) and abluminal (ABL) sides of ISA **(upper panels)** and NASB **(lower panels)** struts. Thickness was measured as the distance from the inner contour of the polymer-neointima interface to the neointima-lumen interface, following a straight line connecting the midpoint of the longitudinal axis of the strut with the center of gravity of the vessel. The correct alignment is achieved using a tool of LightLab's proprietary software named "thickness ruler." This guiding line, however, has been erased from the image to ease its comprehension. Abbreviations as in Figure 1.

Table 2. Baseline Clinical Characteristics of the Patients (N = 28)

Male	23 (82.1)
Age, yrs*	64.5 (56.0–70.4)
Hypertension	15 (53.6)
DM	2 (7.1)
Insulin-requiring	1 (3.6)
Hypercholesterolemia	27 (96.4)
Smoking	5 (17.9)
Family history of CHD	13 (46.4)
Prior	
MI	13 (46.4)
PCI	7 (25.0)
Of the target vessel	2 (7.1)
Clinical indication	
Stable angina	21 (75.0)
Unstable angina	4 (14.3)
No. of diseased vessels	
1	22 (78.6)
2	3 (10.7)
3	3 (10.7)

*Values are n (%) or median (25th percentile to 75th percentile).
CHD = coronary heart disease; DM = diabetes mellitus; MI = myocardial infarction; PCI = percutaneous coronary intervention.

thicker ADL coverage were calculated and compared by pooled analysis using an inverse variance random effects model for paired measurements, taking into account the between-clusters and within-the-cluster variability, using each stent as an independent unit of clustering (30). The odds ratio at each individual stent and the pooled odds ratio of the whole sample were graphically represented by means of forest plots. Results for the whole sample of struts and for the ISA and NASB subgroups were reported. Interobserver variability for measurements at each side of the struts was estimated by intraclass correlation coefficients for the absolute agreement (ICCa).

All the analyses and graphics were performed with the PASW version 17.0.2 (SPSS, Chicago, Illinois) and CMA Version 2 (Biostat, Englewood, New Jersey) software packages.

Results

The average follow-up period for Cohort B1 was 183 ± 9 days. A total of 28 patients (28 lesions and scaffolds, 4,670 struts) were analyzed with OCT. Table 2 shows the baseline clinical characteristics of the patients. Sixteen of 28 analyzed scaffolds presented ISA or NASB struts suitable for the planned comparison: 114 struts (2.4%, 85 ISA and 29 NASB). The reproducibility of the measurements was excellent (ICCa: 0.908, 95% confidence interval [CI]: 0.869 to 0.935 for the ADL side; ICCa: 0.982, 95% CI: 0.975 to 0.988 for the ABL side; with no significant bias detected).

Coverage was significantly thicker on the ABL than on the ADL side in the whole sample (101 μm; 95% CI: 87 to 116 μm vs. 71 μm; 95% CI: 59 to 83 μm; mean difference: 30 μm, 95% CI: 20 to 40 μm; $p < 0.0001$) and in the subgroups of ISA (95 μm; 95% CI: 80 to 111 μm vs. 65 μm; 95% CI: 53 to 76 μm; mean difference: 31 μm, 95% CI: 19 to 43 μm; $p < 0.0001$) and NASB struts (110 μm; 95% CI: 83 to 139 μm vs. 83 μm; 95% CI: 58 to 108 μm; mean difference 30 μm, 95% CI: 20 to 40 μm; $p = 0.008$) (Table 3).

In 70 struts (60.7%, 95% CI: 50.6% to 70.0%), the neointimal coverage was thicker on the ABL side. Conversely, only 20 struts (17.5%) had thicker neointimal coverage on the ADL side ($p < 0.0001$). Similar results were observed in the ISA and NASB subgroups, although in the latter, the difference in

Table 3. Thickness of Neointimal Coverage at the ADL and ABL Sides of the Struts

	Neointimal Thickness (μm)			
		95% CI		
	Mean	Lower	Upper	p Value
All detached struts, n = 114 (16 stents)				
ADL	71	59	83	
ABL	101	87	116	
(ABL − ADL) difference	30	20	40	<0.0001
ISA struts, n = 85 (12 stents)				
ADL	65	53	76	
ABL	95	80	111	
(ABL − ADL) difference	31	19	43	<0.0001
NASB struts, n = 29 (6 stents)				
ADL	83	58	108	
ABL	110	83	139	
(ABL − ADL) difference	28	8	47	0.008

Shown are the weighted average values and paired comparisons (multilevel linear regression for paired measurements).
ABL = abluminal; ADL = adluminal; CI = confidence interval; ISA = incomplete stent apposition; NASB = nonapposed side branch.

Table 4. Percentage of Struts With Neointimal Coverage Thicker on the ABL Than on the ADL Side and Vice Versa

		Pooled %			Paired Comparison			
			95% CI			95% CI		
	n	Estimate	Low	Upper	OR	Low	Upper	p Value
Whole sample, n = 114 struts (16 stents)								
ABL thicker	70	60.7	50.6	70.0	3.35	2.22	5.07	<0.0001
ADL thicker	20	18.5	11.6	28.1				
ISA, n = 85 struts (12 stents)								
ABL thicker	55	64.8	52.9	75.2	4.16	2.53	6.82	<0.0001
ADL thicker	14	18.3	10.4	30.1				
NASB, n = 29 struts (6 stents)								
ABL thicker	15	47.2	28.0	67.3	1.92	0.90	4.12	0.094
ADL thicker	6	20.2	7.8	43.0				

Shown are the pooled estimations of the proportions and the pooled paired comparisons.
OR = odds ratio; other abbreviations as in Table 3.

percentages did not reach statistical significance (Table 4, Fig. 3). In 105 struts (92.1%), the thickness of ABL coverage was >30 μm: 76 (89.4%) ISA struts and 29 (100%) NASB struts, compared with 98 struts (86.0%) in which the ADL thickness was >30 μm: 71 (83.5%) ISA and 27 (93.1%) NASB struts.

Discussion

The main findings of this study are: 1) neointimal coverage is thicker on the ABL than on the ADL side in 61.4% of ISA and NASB struts; and 2) at least 60.7% and up to 92.1% of the ISA and NASB struts are covered on the ABL side after 6 months in the BVS.

To the best of our knowledge, this is the first study comparing in vivo the neointimal thickness on the ADL versus the ABL surface of an intracoronary device in a cohort of patients. This comparison had not been technically possible hitherto for two reasons. First, only struts remaining detached from the vessel wall at follow-up present both ADL and ABL surfaces in which neointimal thickness can be measured. This limits the study to small ISA or side-branch regions, difficult to detect and to track. Second and more importantly, the intense backscattering of the ultrasound or of the optical beam at the metallic struts has prevented visualization of their ABL side in BMS or DES. The translucency of the PLLA polymer in the BVS enables for the first time quantification of the ABL neointimal coverage.

The assessment of coverage in the BVS with OCT is challenging. The translucency of the polymer results in a frame-shaped backscattering at the strut boundaries. This

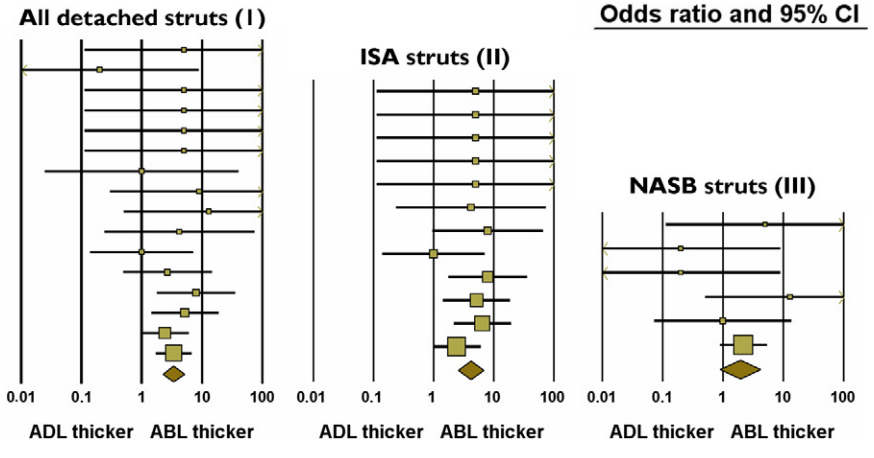

Figure 3. Paired Pooled Comparison of the Percentages of Struts With Thicker Coverage on the ABL Than on the ADL Side Versus the Opposite

Forest plot representing the odds ratio and 95% confidence interval (CI) for each stent and the pooled odds ratio at the **bottom**. Abbreviations as in Figures 1 and 2.

signal convolutes with the one generated by neointima, and they often become indiscernible. We circumvented this limitation by taking the inner contour of the backscattering frame of the strut. Compared with other methods of measurement, this approach offers the advantage of a clear reproducible criterion (P. W. Serruys, Y. Onuma, J. A. Ormiston, et al., unpublished data, June 2010), although it overestimates slightly the neointimal thickness due to the inclusion of the polymer backscattering (~30 μm) in the measurement. Since our current study is based on the relative thickness on one side versus the other, rather than in absolute thickness values, we chose the most accurate and reproducible method of measurement. Our results strongly suggest that most ISA and NASB struts are covered on the ABL side in the BVS at 6 months: at least 60.7%, considering those struts with ABL > ADL thickness, or up to 92.1% if we include also those struts with ABL thickness >30 μm, regardless of the ADL/ABL ratio. Previous OCT studies reported that only 27.4% to 34.6% of ISA struts were covered on the ADL side after 9 to 13 months in metallic DES (24,30). Our observations would suggest that the ABL side might be a more favorable scenario than the ADL for a complete coverage, but this finding could be also explained by differential characteristics of the BVS, since the ADL coverage of ISA struts was also higher in this study than in previous reports on metallic DES (24,30).

The differences in neointimal thickness suggest that the neointimal inhibition is for some reason less efficient on the ABL than on the ADL side. Differences in shear stress (SS) between the ADL and ABL sides might likely play a role to explain this finding. An inverse relation between SS and neointimal hyperplasia has been described in BMS (31) and DES (32–34). Computational models studying the effect of catheter placement (35,36) and of stent infraexpansion (37) on wall SS have consistently found lower SS levels when the catheter was placed close to the vessel wall (35,36) or beneath the struts of an undersized stent (37). Therefore, SS could be lower at the ABL side and thus explain the thicker neointima. Our results fit well into this SS theoretical model, although fluid dynamics can vary considerably depending on the geometry of the vessel, so the hydrodynamic forces become regionally unpredictable. Surprisingly, NASB struts show a similar ADL/ABL thickness ratio to that of ISA struts, although in a bifurcation, both sides can be submitted to high SS forces. Side branches >2-mm diameter were an exclusion criterion for this study, thus our NASB struts correspond predominantly to tiny side branches, probably with flow patterns closer to the ISA scenario than to the true bifurcation. Other factors, such as a more intense wound healing reaction in the vicinity of the vascular tissue, could also play a role.

The neointimal healing on the ABL side is relevant to understand the mechanism by which acute stent malapposition might be spontaneously corrected over time. We have learned from OCT studies that the proportion of malapposed struts gets spontaneously reduced from approximately 7.7% immediately after stenting to 1.2% at 6 months follow-up (25); but the physiological mechanism for this correction is to a great extent unknown, and it is important to understand why it happens in some regions but not in others. The thicker ABL neointima suggests that the integration process of malapposed areas into the vessel wall might be the consequence of neointimal growth from the strut to the vessel or bidirectionally, rather than merely from vessel to strut.

Study limitations. Although the term "neointimal thickness" is commonly used in OCT studies (21,22,38,39), its sensitivity and specificity for neointimal detection are still unknown and <100%. OCT coverage correlates with histological neointima and endothelialization after stenting in animal models (40–43); but OCT is unable to detect thin layers of endothelium below 14-μm axial resolution, and cannot discern between neointima and other material, such as fibrin or thrombus. Optical densitometry analysis might be useful in the future (42). Additionally, OCT has been validated for the assessment of neointimal coverage, taking into account only the ADL coverage. This study has been performed under the assumption that the validation on the ADL side can also apply to the ABL side: this hypothesis, although theoretically plausible, has not been empirically demonstrated to date.

The observations in this study apply only to the BVS, a bioresorbable everolimus-eluting vascular scaffold. Extrapolation of the conclusions to other intracoronary devices, such as BMS or DES, must be cautious, even though considerable analogy has been described in the neointimal healing of these devices.

Conclusions

Most malapposed and side-branch struts are covered on the ABL side 6 months after BVS implantation, with thicker neointimal coverage than on the ADL side. The physiological correction of acute malapposition involves neointimal growth from the strut to the vessel wall or bidirectional.

Reprint requests and correspondence: Prof. Patrick W. Serruys, Erasmus Medical Center, Thoraxcentre, Ba583a, 's-Gravendijkwal 230, 3015 CE Rotterdam, the Netherlands. E-mail: p.w.j.c.serruys@erasmusmc.nl.

REFERENCES

1. Liu MW, Roubin GS, King SB III. Restenosis after coronary angioplasty. Potential biologic determinants and role of intimal hyperplasia. Circulation 1989;79:1374–87.
2. Essed CE, Van den Brand M, Becker AE. Transluminal coronary angioplasty and early restenosis. Fibrocellular occlusion after wall laceration. Br Heart J 1983;49:393–6.
3. Giraldo AA, Esposo OM, Meis JM. Intimal hyperplasia as a cause of restenosis after percutaneous transluminal coronary angioplasty. Arch Pathol Lab Med 1985;109:173–5.

4. Austin GE, Ratliff NB, Hollman J, Tabei S, Phillips DF. Intimal proliferation of smooth muscle cells as an explanation for recurrent coronary artery stenosis after percutaneous transluminal coronary angioplasty. J Am Coll Cardiol 1985;6:369–75.
5. Reidy MA, Standaert D, Schwartz SM. Inhibition of endothelial cell regrowth. Cessation of aortic endothelial cell replication after balloon catheter denudation. Arteriosclerosis 1982;2:216–20.
6. Haudenschild CC, Schwartz SM. Endothelial regeneration. II. Restitution of endothelial continuity. Lab Invest 1979;41:407–18.
7. Reidy MA, Schwartz SM. Endothelial regeneration. III. Time course of intimal changes after small defined injury to rat aortic endothelium. Lab Invest 1981;44:301–8.
8. Björkerud S, Bondjers G. Arterial repair and atherosclerosis after mechanical injury. 5. Tissue response after induction of a large superficial transverse injury. Atherosclerosis 1973;18:235–55.
9. Reidy MA, Clowes AW, Schwartz SM. Endothelial regeneration. V. Inhibition of endothelial regrowth in arteries of rat and rabbit. Lab Invest 1983;49:569–75.
10. Clowes AW, Karnowsky MJ. Suppression by heparin of smooth muscle cell proliferation in injured arteries. Nature 1977;265:625–6.
11. Kong D, Melo LG, Gnecchi M, et al. Cytokine-induced mobilization of circulating endothelial progenitor cells enhances repair of injured arteries. Circulation 2004;110:2039–46.
12. Werner N, Kosiol S, Schiegl T, et al. Circulating endothelial progenitor cells and cardiovascular outcomes. N Engl J Med 2005;353:999–1007.
13. Joner M, Finn AV, Farb A, et al. Pathology of drug-eluting stents in humans: delayed healing and late thrombotic risk. J Am Coll Cardiol 2006;48:193–202.
14. Finn AV, Joner M, Nakazawa G, et al. Pathological correlates of late drug-eluting stent thrombosis: strut coverage as a marker of endothelialization. Circulation 2007;115:2435–41.
15. Virmani R, Guagliumi G, Farb A, et al. Localized hypersensitivity and late coronary thrombosis secondary to a sirolimus-eluting stent: should we Be cautious? Circulation 2004;109:701–5.
16. Farb AM, Burke APM, Kolodgie FDP, Virmani RM. Pathological mechanisms of fatal late coronary stent thrombosis in humans. Circulation 2003;108:1701–6.
17. Awata M, Kotani J, Uematsu M, et al. Serial angioscopic evidence of incomplete neointimal coverage after sirolimus-eluting stent implantation: comparison with bare-metal stents. Circulation 2007;116:910–6.
18. Awata M, Nanto S, Uematsu M, et al. Angioscopic comparison of neointimal coverage between zotarolimus- and sirolimus-eluting stents. J Am Coll Cardiol 2008;52:789–90.
19. Takano M, Ohba T, Inami S, Seimiya K, Sakai S, Mizuno K. Angioscopic differences in neointimal coverage and in persistence of thrombus between sirolimus-eluting stents and bare metal stents after a 6-month implantation. Eur Heart J 2006;27:2189–95.
20. Barlis P, Regar E, Serruys PW, et al. An optical coherence tomography study of a biodegradable vs. durable polymer-coated limus-eluting stent: a LEADERS trial sub-study. Eur Heart J 2010;31:165–76.
21. Guagliumi G, Sirbu V, Musumeci G, et al. Strut coverage and vessel wall response to a new-generation paclitaxel-eluting stent with an ultrathin biodegradable abluminal polymer: Optical Coherence Tomography Drug-Eluting Stent Investigation (OCTDESI). Circ Cardiovasc Interv 2010;3:367–75.
22. Guagliumi G, Sirbu V, Bezerra H, et al. Strut coverage and vessel wall response to zotarolimus-eluting and bare-metal stents implanted in patients with ST-segment elevation myocardial infarction: the OCTAMI (Optical Coherence Tomography in Acute Myocardial Infarction) study. J Am Coll Cardiol Intv 2010;3:680–7.
23. Guagliumi G, Costa MA, Sirbu V, et al. Strut coverage and late malapposition with paclitaxel-eluting stents compared with bare metal stents in acute myocardial infarction: optical coherence tomography substudy of the Harmonizing Outcomes With Revascularization and Stents in Acute Myocardial Infarction (HORIZONS-AMI) trial. Circulation 2011;123:274–81.
24. Ozaki Y, Okumura M, Ismail TF, et al. The fate of incomplete stent apposition with drug-eluting stents: an optical coherence tomography-based natural history study. Eur Heart J 2010;31:1470–6.
25. Gutiérrez-Chico JL, van Geuns RJ, Koch KT, et al. Paclitaxel-coated balloon in combination with bare metal stent for treatment of de novo coronary lesions: an optical coherence tomography first-in-human randomized trial balloon-first vs. stent first. EuroIntervention 2011;7:711–22.
26. Gutiérrez-Chico JL, Jüni P, García-García HM, et al. Long term tissue coverage of a biodegradable polylactide polymer-coated biolimus-eluting stent: comparative sequential assessment with optical coherence tomography until complete resorption of the polymer. Am Heart J 2011;162:922–31.
27. Serruys PW, Ormiston JA, Onuma Y, et al. A bioabsorbable everolimus-eluting coronary stent system (ABSORB): 2-year outcomes and results from multiple imaging methods. Lancet 2009;373:897–910.
28. Ormiston JA, Serruys PW, Regar E, et al. A bioabsorbable everolimus-eluting coronary stent system for patients with single de-novo coronary artery lesions (ABSORB): a prospective open-label trial. Lancet 2008; 371:899–907.
29. Serruys PW, Onuma Y, Ormiston JA, et al. Evaluation of the second generation of a bioresorbable everolimus drug-eluting vascular scaffold for treatment of de novo coronary artery stenosis: six-month clinical and imaging outcomes. Circulation 2010;122:2301–12.
30. Gutiérrez-Chico JL, Regar E, Nüesch E, et al. Delayed coverage in malapposed and side-branch struts with respect to well-apposed struts in drug-eluting stents: in vivo assessment with optical coherence tomography. Circulation 2011;124:612–23.
31. Wentzel JJ, Krams R, Schuurbiers JC, et al. Relationship between neointimal thickness and shear stress after Wallstent implantation in human coronary arteries. Circulation 2001;103:1740–5.
32. Gijsen FJH, Oortman RM, Wentzel JJ, et al. Usefulness of shear stress pattern in predicting neointima distribution in sirolimus-eluting stents in coronary arteries. Am J Cardiol 2003;92:1325–8.
33. Tanabe K, Gijsen FJH, Degertekin M, et al. True three-dimensional reconstructed images showing lumen enlargement after sirolimus-eluting stent implantation. Circulation 2002;106:e179–80.
34. Thury A, Wentzel JJ, Vinke RVH, et al. Focal in-stent restenosis near step-up: roles of low and oscillating shear stress? Circulation 2002;105:e185–7.
35. Wentzel JJ, Krams R, van der Steen AFW, et al. Disturbance of 3D velocity profiles induced by an IVUS catheter: evaluation with computational fluid dynamics. Comput Cardiol 1997;24:597–600.
36. Krams R, Wentzel JJ, Cespedes I, et al. Effect of catheter placement on 3-D velocity profiles in curved tubes resembling the human coronary system. Ultrasound Med Biol 1999;25:803–10.
37. Chen HY, Hermiller J, Sinha AK, Sturek M, Zhu L, Kassab GS. Effects of stent sizing on endothelial and vessel wall stress: potential mechanisms for in-stent restenosis. J Appl Physiol 2009;106:1686–91.
38. Miyoshi N, Shite J, Shinke T, et al. Comparison by optical coherence tomography of paclitaxel-eluting stents with sirolimus-eluting stents implanted in one coronary artery in one procedure: 6-month follow-up. Circ J 2010;74:903–8.
39. Takano M, Yamamoto M, Mizuno M, et al. Late vascular responses from 2 to 4 years after implantation of sirolimus-eluting stents: serial observations by intracoronary optical coherence tomography. Circ Cardiovasc Interv 2010;3:476–83.
40. Prati F, Zimarino M, Stabile E, et al. Does optical coherence tomography identify arterial healing after stenting? An in vivo comparison with histology, in a rabbit carotid model. Heart 2008;94:217–21.
41. Murata A, Wallace-Bradley D, Tellez A, et al. Accuracy of optical coherence tomography in the evaluation of neointimal coverage after stent implantation. J Am Coll Cardiol Img 2010;3:76–84.
42. Templin C, Meyer M, Müller MF, et al. Coronary optical frequency domain imaging (OFDI) for in vivo evaluation of stent healing: comparison with light and electron microscopy. Eur Heart J 2010;31:1792–801.
43. Onuma Y, Serruys PW, Perkins LE, et al. Intracoronary optical coherence tomography and histology at 1 month and 2, 3, and 4 years after implantation of everolimus-eluting Bioresorbable vascular scaffolds in a porcine coronary artery model: an attempt to decipher the human optical coherence tomography images in the ABSORB trial. Circulation 2010;122:2288–300.

Key Words: drug-eluting stent(s) ■ neointima ■ optical coherence ■ poly(lactide) ■ tomography.